Journal of Solid State Chemistry **162,** 371–378 (2001)
doi:10.1006/jssc.2001.9326, available online at http://www.idealibrary.com on IDEAL®

Modifying Silica Xerogels by Fluoride-Ion-Catalyzed Chemical Treatment

Valérie Le Strat, Bruno Boury, and Robert J. P. Corriu[1]

Laboratoire de Chimie Moléculaire et Organisation du Solide, UMR 5637, Université Montpellier II, Place E. Bataillon, 34095 Montpellier Cedex 5, France

and

Pierre Delord

Groupe de Dynamique des Phases Condensées, UMR 5581, Université Montpellier II, Place E. Bataillon, 34095 Montpellier Cedex 5, France

THIS PAPER IS DEDICATED TO PROFESSOR PAUL HAGENMULLER IN RECOGNITION OF HIS OUTSTANDING CONTRIBUTION TO SOLID STATE CHEMISTRY AND MATERIAL SCIENCE, AND HIS TREMENDOUS IMPACT ON THE DEVELOPMENT OF CHEMISTRY IN FRANCE

INTRODUCTION

In the course of our studies concerning the nanostructured hybrid organic–inorganic materials, we have focused on materials obtained by the hydrolytic polycondensation of molecular precursors in which the organic unit is covalently attached to at least two $-Si(OR)_3$ groups (Scheme 1) (1, 2). The sol–gel type reaction of $-Si(OR)_3$ groups leads to the synthesis of a macromolecular polysilsequioxane which corresponds to a Si–O–Si amorphous network in which the organic units are covalently bound to silicon.

We have previously developed a chemical method for the elimination of organic units in nanostructured hybrids using NH_4F as catalyst (Scheme 1) (3–6). The Si–C bond cleavage induced in this way leads to a siliceous residue which exhibits a very narrow distribution of pore diameters. A SAXS (small-angle X-ray scattering) study of the silica always shows a Porod surface, with a good agreement between porosimetry and SAXS methods for the determination of the size of the pores. In contrast, the thermal elimination of the organic units always provided a wider pore size diameter distribution in a range of lower diameters. All these experimental facts suggested an effect of the F^- catalyst on the Si–O–Si network which was evidenced by the drastic influence of this nucleophile on both the specific surface area and porosity (7). It is well known in the silicon chemistry performed in solution that F^- is a very efficient catalyst for many reactions occurring at silicon (8–10). In other words, the catalyst used for the Si–C bonds breaking also has the possibility to induce other reactions like polycondensation by Si–O–Si bond formation and reorganization of the SiO_2 network by Si–O–Si redistribution.

It was very attractive to check this possible method of solid reorganization in the case of SiO_2 independently of the presence of any organic groups. In this paper we describe the F^--induced chemical treatment of silica samples obtained by sol–gel type hydrolysis of tetramethoxysilane under different conditions. All these samples have been submitted to the same experimental conditions and have been studied considering polycondensation at silicon and porosity variations by porosimetry and SAXS measurements.

RESULTS

Preparation and Treatment of Silica Xerogels

The starting silica xerogels were prepared by sol–gel hydrolysis/polycondensation of 3 M solutions of tetramethoxysilane (TMOS) in EtOH, MeOH, or THF with a stoichoimetric amount of water and using HCl or NH_4OH as catalyst (catalyst/TMOS molar ratio 1%). The gelation times vary from a few minutes for the gels prepared under basic conditions to 2 months for the gels prepared under acidic conditions. The gels were then processed and dried at 100°c for 24 hours under vacuum (Scheme 2).

The silica xerogels ($\mathbf{S_{1-6}}$) were treated in a water/methanol/NH_4F mixture at reflux for 4 days. The treated silica $\mathbf{ST_{1-6}}$ are recovered after filtration, washing, and drying. In the cases of $\mathbf{S_3}$ and $\mathbf{S_4}$ the same treatment was performed in the absence of NH_4F leading to silica xerogels $\mathbf{ST'_3}$ and $\mathbf{ST'_4}$.

[1]To whom correspondence should be addressed.

0022-4596/01 $35.00

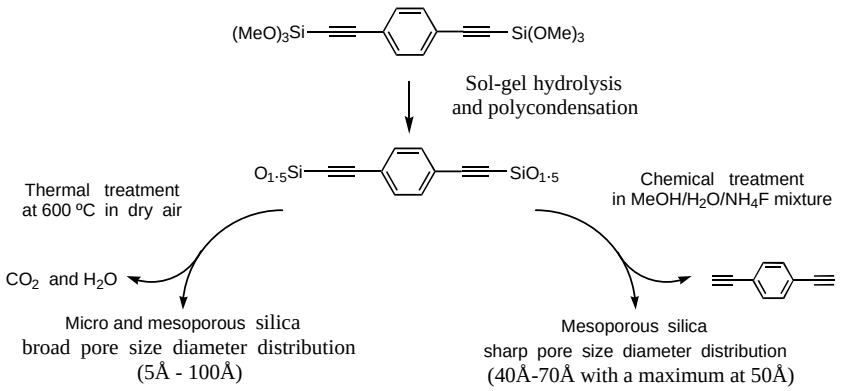

SCHEME 1. Chemical and thermal treatment of hybrid xerogels: access to porous silica.

^{29}Si Solid State NMR Analysis

All the solid NMR spectra were obtained using the CP MAS sequence; it does not allow a precise quantitative determination of the level of condensation but comparison between materials before and after treatment can be used for qualitative measurements.

Three signals are observed corresponding to the three types of silicon atom environments: Q^2 (-94 ppm), Q^3 (-100 ppm), and Q^4 (-110 ppm). No Q^0 (TMOS) or Q^1 signals were observed (Table 1) (11, 12). In every case, the Q^3 signal represents the highest intensity, Q^2 and Q^4 signals both having lower intensities than Q^3 (Fig. 1a). Xerogels $\mathbf{S_2}$ (EtOH, HCl) and $\mathbf{S_1}$ (EtOH, NH_3) present the highest condensation level.

After chemical treatment, an increase of the Q^4 signal and a decrease of the Q^2 signal are observed for all the xerogels $\mathbf{ST_{1-6}}$. As an example NMR data of $\mathbf{S_3}$ and $\mathbf{ST_3}$ are given and illustrate these variations of signals' intensity (Figs. 1a and 1c). Both phenomena lead to an increase of the condensation level. This trend is observed for all the materials but

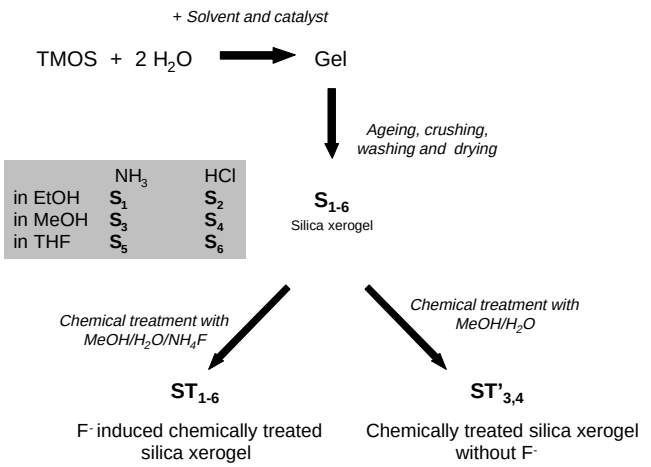

SCHEME 2. S_{1-6} xerogels: preparation and treatment.

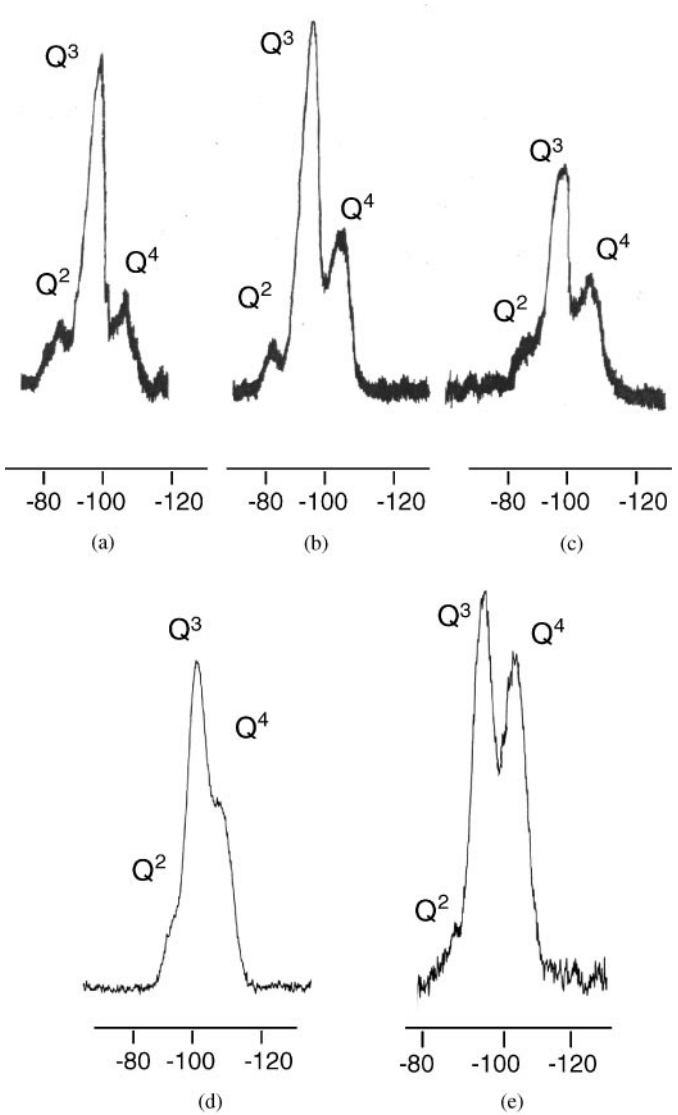

FIG. 1. ^{29}Si CP MAS solid state NMR spectra of (a) $\mathbf{S_3}$, (b) $\mathbf{ST'_3}$, (c) $\mathbf{ST_3}$, (d) $\mathbf{S_2}$, and (e) $\mathbf{ST_2}$.

TABLE 1
Chemical Shifts for the Silica Q^n Signals

Silica environment	Q^{0a}	Q^{1a}	Q^2	Q^3	Q^4
Chemical shift (ppm)	−79	−86	−94	−100	−110

[a] Signals not observed experimentally.

with various intensity. We found that correlation with other characteristics, such as specific surface area, is not possible. Indeed, an increase of the polycondensation level is also observed for materials with very low specific surface area like in the case of $\mathbf{S_2}$ leading to $\mathbf{ST_2}$. This may indicate a transformation not limited to the surface of the solid.

These transformations of the silica xerogels upon chemical treatment are also observed in the case of the chemical treatment without fluoride ion but apparently the variations are lower, as illustrated by comparison of $\mathbf{ST_3}$ and $\mathbf{ST'_3}$ (Figs. 1b and 1c).

Gas Adsorption Porosimetry

The porosity of the solid was characterized by porosimetry measurements with N_2. We verified that the results did not vary over time by repeating the measurements after 6 months on each samples. No modification was observed although the samples were not stored under nitrogen.

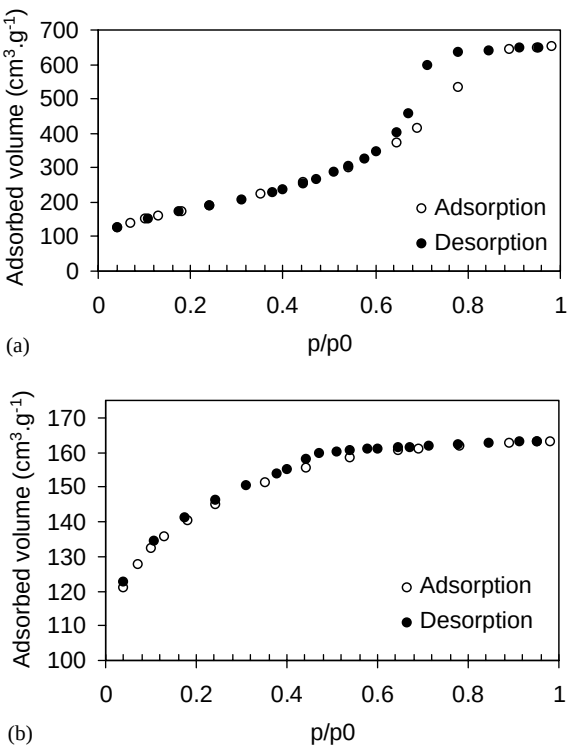

FIG. 2. Isotherm plots of (a) $\mathbf{ST_3}$ and (b) $\mathbf{S_6}$.

TABLE 2
Porosimetry Measurements for the Xerogels before and after Treatment

	Specific surface area ($m^2 \cdot g^{-1}$)		Mean pore diameter (Å) (half-peak width (Å))	
	Before chemical treatment	After chemical treatment	Before chemical treatment	After chemical treatment
		Basic Condition		
EtOH, NH_3	$\mathbf{S_1}$:700	$\mathbf{ST_1}$:590	$\mathbf{S_1}$:80 (40)	$\mathbf{ST_1}$:100 (60)
MeOH, NH_3	$\mathbf{S_3}$:650	$\mathbf{ST_3}$:300	$\mathbf{S_3}$:65 (15)	$\mathbf{ST'_3}$:200 (> 100)
		$\mathbf{ST'_3}$:420		$\mathbf{ST'_3}$:100 (65)
THF, NH_3	$\mathbf{S_5}$:490	$\mathbf{ST_5}$:360	$\mathbf{S_5}$:200 (150)	$\mathbf{ST_5}$:200 (180)
		Acidic Condition		
MeOH, HCl	$\mathbf{S_4}$: < 10	$\mathbf{ST_4}$: < 10	—	—
		$\mathbf{ST'_4}$: < 10		
EtOH, HCl	$\mathbf{S_2}$: < 10	$\mathbf{ST_2}$: < 10	—	—
THF, HCl	$\mathbf{S_6}$:460	$\mathbf{ST_6}$:80	$\mathbf{S_6}$:15 (5)	$\mathbf{ST_6}$:35 (10)

For the xerogels prepared with a basic catalyst, a type IV isotherm plot was obtained, with a hysteresis of H1 type (IUPAC), characteristic of mesoporous materials with cylindrical or ink-bottle-shaped pores. This was observed for the starting xerogels $\mathbf{S_1}$, $\mathbf{S_3}$, and $\mathbf{S_5}$ but also for those after chemical treatment, $\mathbf{ST_1}$, $\mathbf{ST_3}$, $\mathbf{ST'_3}$, and $\mathbf{ST_5}$ (Fig. 2a). For these solids a high specific surface area is measured and the chemical treatment leads to a lowering of these values (15%, 55%, and 25%, respectively, for $\mathbf{ST_1}$, $\mathbf{ST_3}$, and $\mathbf{ST_5}$) (Table 2). A decrease of the specific surface area is also observed when the treatment is performed in the absence of F^- anions ($\mathbf{ST'_3}$); however, the decrease is lower than with fluoride ions ($\mathbf{ST_3}$).

The xerogels prepared under acidic conditions are all nonporous solids ($\mathbf{S_2}$, $\mathbf{S_4}$, $\mathbf{ST_2}$, $\mathbf{ST_4}$, and $\mathbf{ST'_4}$) (type II isotherm plot) with the exception of $\mathbf{S_6}$ which is microporous (Fig. 2b). In this last case the *t*-plot method shows a microporous volume of 0.19 $cm^3 \cdot g^{-1}$ for $\mathbf{S_6}$. This microporous volume disappears upon chemical treatment and $\mathbf{ST_6}$ is mesoporous. Simultaneously a dramatic decrease of the specific area is observed (−80%). For the nonporous xerogels ($\mathbf{S_2}$, $\mathbf{S_4}$), the chemical treatment does not lead to significant variation of the porosity ($\mathbf{ST_2}$, $\mathbf{ST_4}$, and $\mathbf{ST'_4}$).

The mean pore diameter distribution was evaluated by calculating the half-peak width of the pore diameter distribution plot (Fig. 3). For the xerogels prepared using basic conditions ($\mathbf{S_1}$, $\mathbf{S_3}$, and $\mathbf{S_5}$), the F^--induced chemical treatment leads to an important widening of this plot, giving a large disparity of the pore sizes. This is also observed when the chemical treatment is performed without fluoride ions ($\mathbf{ST'_3}$). An increase of the half-peak width is also observed for $\mathbf{S_6}$ prepared under acidic conditions.

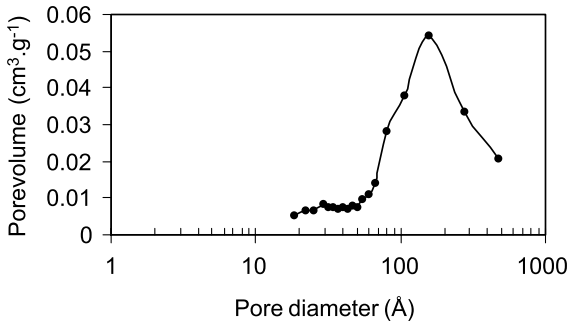

FIG. 3. Example of pore distribution plot for a mesoporous $\mathbf{ST_3}$.

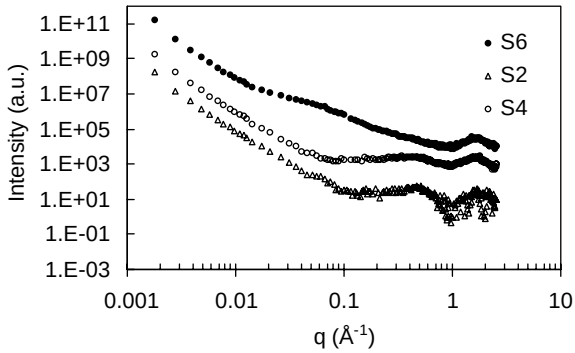

FIG. 4. SAXS diffractograms of xerogels $\mathbf{S_2}$, $\mathbf{S_4}$, and $\mathbf{S_6}$.

SAXS Measurements

The powder diffractograms were recorded using high resolution ($0.001 < q < 0.1\,\text{Å}^{-1}$) and low resolution ($0.1 < q < 0.4\,\text{Å}^{-1}$); this allowed us to study the q domain from 0.001 to $0.4\,\text{Å}^{-1}$.

Under basic conditions diffractograms of the xerogels prepared in EtOH ($\mathbf{S_1}$) and MeOH ($\mathbf{S_3}$) present a Porod behavior which is also observed after chemical treatment of the xerogel, with or without fluoride anion. For $\mathbf{S_5}$ prepared in THF, the slope is -3.7 and here also the chemical treatment apparently does not deeply modify this characteristic (Table 3). Apparently the surface of these xerogels prepared under basic condition is "stable" enough under the conditions used for the chemical treatment.

Things are different for the xerogels prepared under acidic conditions. Here, a power law was determined for $\mathbf{S_2}$, $\mathbf{S_4}$, and $\mathbf{S_6}$ in the q domain $0.003 < q < 0.03\,\text{Å}^{-1}$ (Fig. 4). For $\mathbf{S_2}$ and $\mathbf{S_4}$, the power law can be related to a fractal dimension indicating a bushy surface of the powder. The xerogels $\mathbf{S_2}$ and $\mathbf{S_4}$ present a wide signal centered around $0.5\,\text{Å}^{-1}$ ($d \approx 12$ Å), one explanation being the presence of a close microporosity not accessible by the nitrogen adsorption measurements. We also found a clear difference between nonporous $\mathbf{S_{2-4}}$ and microporous $\mathbf{S_6}$ when looking at the $0.4 < q < 2.5\,\text{Å}^{-1}$ domain; however, this difference is difficult to interpret and may be related to interpore interactions and porosity distribution.

Concerning the chemical treatment of these materials, the main feature is the decrease of the slope in the Porod region that leads for $\mathbf{ST_2}$ and $\mathbf{ST_4}$ to a Porod behavior (Table 3). Focusing on the case of $\mathbf{S_2/ST_2}$ (Fig. 5), we found that this nonporous material exhibits by SAXS measurement a power law of -3.5 and a broad signal in the Bragg domain (12 Å). After chemical treatment a "classical" Porod behavior is observed and a Guinier plateau allows the determination of $\xi \approx 20$ Å. This spectacular variation induced by the chemical treatment may result from the transformation of the solid with a closed microporosity and surface fractal behavior ($D_s = 2.5$) into a nonporous silica xerogel with a clear-cut interface. The effect of the F^- anion apparently corresponds to a reorganization of the aggregates that requires cleavage and reorganization of the Si–O–Si bonds.

For $\mathbf{S_6/ST_6}$ the same variations due to chemical treatment are observed but seem to be more limited (from -2.5 to -3.0). A plateau in the Guinier region was clearly observed in this case, the bump around $q = 0.03\,\text{Å}^{-1}$ corresponding to a calculated elementary particle size of $\xi \approx 30$ Å.

TABLE 3
Slopes in the Porod Domain

	Power law, the Porod region	
	Before chemical treatment	After chemical treatment
$\mathbf{S_1/ST_1}$	-4	-4
$\mathbf{S_2/ST_2}$	-3.5 ($D_s = 2.5$)	-4
$\mathbf{S_3/ST_3/ST_3'}$	-4	-4; -4
$\mathbf{S_4/ST_4/ST_4'}$	-3.8 ($D_s = 2.2$)	-4; -2.7 ($D_s = 3.3$[a])
$\mathbf{S_5/ST_5}$	-3.7 ($D_s = 2.3$)	-3.6 ($D_s = 2.4$)
$\mathbf{S_6/ST_6}$	-2.5 ($D_s = 3.5$[a])	-3.0 ($D_s = 3$)

[a] D_s value must be between 2 and 3; these values do not have any physical meaning.

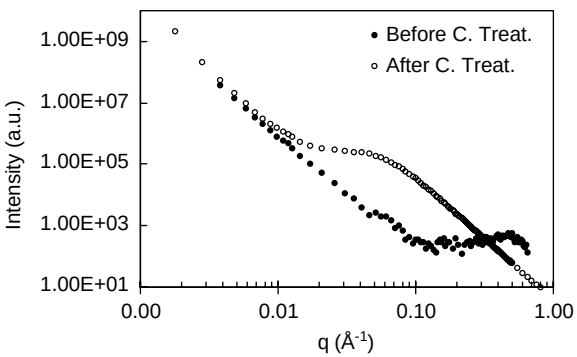

FIG. 5. SAXS diffractograms for $\mathbf{S_2}$ and $\mathbf{ST_2}$.

Porosimetry by SAXS Measurement

Plotting $\ln(q^4 I) = f(q)$ emphasizes the variations in the Porod region. The absence of oscillations on these plots reveals the polydispersity of the clusters sizes. The asymptotic Porod behavior allows us to determine two parameters, K and Q, respectively the Porod's limit and invariant (13). This type of calculation was done on $\mathbf{S_1/ST_1}$ and $\mathbf{S_3/ST_3}$ materials that present a Porod behavior. According to the hypothesis of a porous material, we used the solid phase density ρ_s and volume fraction φ_s, and the gaseous phase volume fraction φ_p (ρ_p being equal to 0) in order to calculate an average cut length $\bar{l}$, by the Eq. [1] and ultimately the parameters $\bar{l}_s$, $\bar{l}_p$ with Eqs. [2]–[4]:

$$\bar{l} = AQ(\pi K)^{-1} \quad [2]$$

$$\bar{l}^{-1} = \bar{l}_s^{-1} + \bar{l}_p^{-1} \quad [3]$$

$$\bar{l} = \varphi_p \bar{l}_s = \bar{l}_p \varphi_s. \quad [4]$$

$\bar{l}_s$ and $\bar{l}_p$ are the average cut length respectively in the solid and in the gas. Using these parameters, the specific surface area S_p can be calculated using Eq. [5]:

$$S_p = 10^4 \pi K \varphi_p (Q\rho_s)^{-1}. \quad [5]$$

The determination of φ_s requires generally monoliths like those obtained for aerogels. However, in the present case the porosimetry analyses allow us to measure the porous volume and consequently the solid volume, considering that all the pores are accessible.

Thus φ_p and φ_s are taken from the porosimetry measurement and used for the calculation of $\bar{l}_p$, $\bar{l}_s$, and S_p. Good agreement between the specific surface area determined by porosimetry and S_p determined by SAXS verifies the compatibility of the two methods. Similarly, $\bar{l}_p$ can be assimilated and is expected to be identical to the average pore radius determined by porosimetry. The $\bar{l}_s$ value represents the average material thickness of the solid phase between two solid/air interfaces.

The specific area measured by porosimetry and S_p values calculated by SAXS are quite similar, indicating the absence of closed porosity (Table 4). The pore diameters obtained by porosimetry and the l_p values are similar, which is confirmation of the absence of closed porosity. Interestingly, we found that the l_s values double in the case of the chemical treatment of $\mathbf{S_3}$ but remain unchanged in the case of $\mathbf{S_1/ST_1}$.

TABLE 4
Comparison of S_p to the Porosimetry Values

	S_p[a] ($m^2 \cdot g^{-1}$)	Specific area[b] ($m^2 \cdot g^{-1}$)	l_s (Å)	l_p (Å)	Mean pore diameter[b] (Å)
$\mathbf{S_1/ST_1}$	630/650	700/590	31/29	82/90	80/100
$\mathbf{S_3/ST_3}$	580/200	650/300	34/96	70/68	65/55

[a] SAXS measurement; [b] Porosimetry measurement.

TABLE 5
$E_{0.6}$ of the Xerogels before and after Chemical Treatment

	$E_{0.6}$		Variation before and after chemical treatment	
Preparation conditions	Before chemical treatment	After chemical treatment	Specific surface area	$E_{0.6}$
$\mathbf{S_1/ST_1}$	0.15	0.11	−15	−27
$\mathbf{S_2/ST_2}$	0.12	0.11	0	−8
$\mathbf{S_3/ST_3/ST'_3}$	0.24	0.14; 0.11	−55	−46; −54
$\mathbf{S_4/ST_4/ST'_4}$	0.13	0.13; 0.13	0	0
$\mathbf{S_5/ST_5}$	0.20	0.11	−25	−45
$\mathbf{S_6/ST_6}$	0.22	0.12	−84	−45

Hydrophilicity Measurements

The hydrophilicity of the materials was estimated by measuring the adsorption of water. The weight increase due to water absorption of 1.0 g of a dry and degassed solid is noted $E_{0.6}$, and this is related to the presence of residual groups that can bind water molecules at the surface of the material. Results from Table 5 clearly indicate that the hydrophilicity always diminished after chemical treatment, demonstrating the lowering of the adsorption property of the solids toward water. Since the adsorption is a phenomenon occurring mainly at the surface of the solid and facilitated by the presence of silanols, the $E_{0.6}$ decrease is certainly related to the decrease of the specific surface area that is observed. However, because this decrease is not proportional to the specific area decrease, important modifications of the surface are certainly produced by the chemical treatment in such a way that Si–OH is removed from the surface and replaced by a more hydrophobic group like Si–O–Si (condensation between two silanols or a Si–OR bond (esterification).

DISCUSSION

As a general behavior, an increase of the condensation level, a decrease of the specific area, a decrease of the hydrophilicity, and a smoothing of the silica/air interface result from the chemical treatment of silica xerogel by a methanol/water/F^- mixture. However, besides these general trends, three main observations must be made.

First, variations are observed depending on the characteristics of the starting materials, which do not behave identically when submitted to the chemical treatment. For example, variation of the power law in the Porod domain is more important for $\mathbf{S_2}$ prepared under acidic conditions (-3.5 to -4) than for $\mathbf{S_5}$ prepared in basic conditions (-3.7

to -3.6). Similarly, variations of the specific surface area are different even when comparing gels prepared under the same basic condition: for $\mathbf{S_3}$ the chemical treatment introduces a decrease of 55% of the specific surface area while for S_5 the variation is limited to a drecrease of 25%. This emphasizes the role of the porosity of the initial xerogel that depends on the conditions of hydrolysis and polycondensation.

Second, NMR data and porosimetry data reveal that modifications of the polycondensation level at silicon introduced by the chemical treatment are not limited to the surface phenomenon, since variations of the silicon intensities of Q^2, Q^3, and Q^4 signals are observed even in the case of silica xerogels with very low specific surface area, for example $\mathbf{S_2}$.

Third, we observed that variations of the porosimetry characteristics are not correlated with SAXS analyses. For example, a decrease of the specific surface area and an increase of the pores are observed both for $\mathbf{S_1}$ and $\mathbf{S_6}$. At the same time variation of the power law in the Porod domain is important for $\mathbf{S_6}$ (-2.5 for $\mathbf{S_6}$ and -3 for $\mathbf{ST_6}$) while it is the same for $\mathbf{S_1}$ and $\mathbf{ST_1}$.

However, we can conclude that the chemical treatment of silica gels by NH_4F in the presence of methanol and water produces an evolution of the materials with a general trend corresponding to an increase of the polycondensation level at silicon, an increase of the size of the pore, and a change of the shape of the pore for reaching the Porod type surface.

This evolution is catalytically induced by the fluoride ion which is known as a very efficient catalyst for many chemical reactions. One possible explanation for the evolution of the silica surface could be the reorganization of the Si–O–Si bonds occurring at the surface of the SiO_2 and induced by F^-. The redistribution reaction occurring at silicon and induced by nucleophilic activation (F^- for instance) is a well-documented reaction in solution (9). At the surface of the solid F^- could react by coordination at silicon inducing a redistribution of Si–O–Si bonds around the silicon atoms, as presented in Scheme 3.

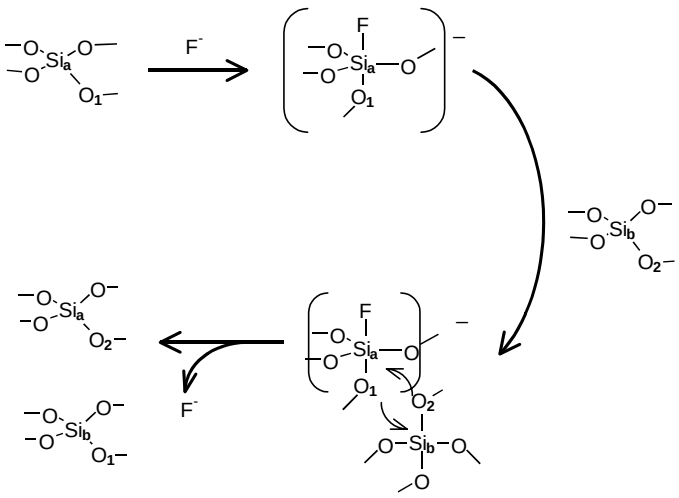

SCHEME 3. Mechanism of the Si–OR functions redistribution catalyzed by the fluoride ions.

The polycondensation at silicon can also be activated by F^-. This explanation could be an alternative to the classical explanation involving redissolution and precipitation of silica units which can also be activated by F^- (14). Both account for the modification of the surface with a thermodynamically controlled evolution.

CONCLUSION

The characteristics of a silica xerogel (mainly condensation rate and porosity) are clearly modified by a water–methanol–fluoride ions-based chemical treatment. We can propose processes each favored by fluoride ions and able to lead to these modifications: polycondensation at silicon, redistribution of Si–O–Si, and redissolution/precipitation of silica colloids.

It is also important to note that the modifications brought to a silica by the chemical treatment can be more or less important depending on the characteristics of the starting silica. This difference can be important, mostly in terms of reagent accessibility, surface reactivity, and porosity.

These results shed a new light on the chemical treatment of hybrid materials. They illustrate that the fluoride ion involves siloxane network modifications that can explain the characteristic modifications observed after elimination of the organic part of the hybrid materials (3–5, 7).

EXPERIMENTAL SECTION

General Conditions

^{29}Si NMR spectra were recorded on an AM300 at 59.620 MHz; 10 s acquisition time, 2 ms contact time, 7400 scans, and 5000 Hz rotating speed were used. Chemical shifts are indicated in ppm referenced to TMS. Porosimetry measurements were performed on either a Micromeritics Gemini III or a Micromeritics ASAP 2010 porosimeter using N_2 at 77 K as adsorbent. The equilibrium time was set to 5 s. Specific area was calculated using the BET equation. Mesoporous distribution was calculated by BJH's method by applying the Harkins and Jura equation. Microporous distribution was obtained using the Horvath–Kawazoe method with the Saito–Foley equation. Microporous volume calculation was performed using the *t*-plot method. Samples were outgassed at 100°C under a 0.1 mmHg vacuum before analysis. High-resolution SAXS analyses were performed on two germanium channel cut apparatuses, where the beam gives three reflections on the (111) planes of each crystal. At low resolution, a classic apparatus was used, with a Ge (111) monochromator and a linear detector for q values less than 0.03 Å^{-1}. Wavelength was 1.542 Å (Cu$K\alpha$ *radiation*). Samples were crushed before analysis. Hydrophilicity measurements were performed on samples

TABLE 6
Gelation Times and Yields for the Xerogels S_{1-6}

Xerogel	Gelation time (min)	Mass of xerogel obtained (g)	Yield (%)
S_1	10	2.07	77
S_2	86×10^3	2.35	87
S_3	1	1.88	70
S_4	86×10^3	2.13	79
S_5	10	1.71	63
S_6	26×10^3	2.24	83

previously dried during 24 hours at 100°C under a 0.1 mmHg vacuum. Hydrophilicity was then measured in a desicrator containing a saturated aqueous NaBr solution (60% humidity rate at equilibrium).

Silica Xerogels Preparation

Tetramethoxysilane (7.0 mL; 49.3 mmol) and solvent (16.0 mL) were mixed with catalyst (1.0 mmol) and water (2 equiv, 98.7 mmol, pH 7). The mixture was stirred until a homogeneous solution was obtained and gelified during stirring. Gel was left for aging for 1 week under ambient temperature (22°C), and then crushed, washed five times with 20.0 mL of ethylic ether, and dried under vacuum at 100°C for 24 hours to give a white powder. For mass and yield (calculated for SiO_2) see Table 6.

Silica Xerogels Characterization

S_1 (EtOH, NH_3). IR (KBr): 956, 1082, 1213, 2997, 3422 cm^{-1}. NMR CP-MAS ^{29}Si δ: -101 (Q^3), −110 (Q^4) ppm. Porosimetry (nitrogen, 77 K). Specific area: 700 $m^2 \cdot g^{-1}$. Mean pore diameter: 80 Å. SAXS: Porod behavior. $S_p = 630\ m^2 \cdot g^{-1}$. $l_s = 31$. $l_p = 82$. $E_{0.6} = 0.15$.

S_2 (EtOH, HCl) IR (KBr): 935, 1087, 1196, 3466 cm^{-1}. NMR CP-MAS ^{29}Si δ: −99 (Q^3), −106 (Q^4) ppm. Porosimetry (nitrogen, 77 K). Specific area: 5 $m^2 \cdot g^{-1}$. SAXS: power law, −3.5; $D_s = 2.5$. $E_{0.6} = 0.12$.

S_3 (MeOH, NH_3). IR (KBr): 969, 1073, 1175, 2855, 3730 cm^{-1}. NMR CP-MAS ^{29}Si δ: −91 (Q^2), −100 (Q^3), −110 (Q^4) ppm. Porosimetry (nitrogen, 77 K). Specific area: 650 $m^2 \cdot g^{-1}$. Mean pore diameter: 65 Å. SAXS: Porod behavior. $S_p = 580\ m^2 \cdot g^{-1}$. $l_s = 34$. $l_p = 70$. $E_{0.6} = 0.24$.

S_4 (MeOH, HCl). IR (KBr): 940, 1087, 1224, 3488 cm^{-1}. NMR CP-MAS ^{29}Si δ: −90 (Q^2), −101 (Q^3), −110 (Q^4) ppm. Porosimetry (nitrogen, 77 K). Specific area: 5 $m^2 \cdot g^{-1}$. SAXS: power law, −3.8; $D_s = 2.2$. $E_{0.6} = 0.13$.

S_5 (THF, NH_3). IR (KBr): 957, 1104, 1213, 2979, 3673 cm^{-1}. NMR CP-MAS ^{29}Si δ: −92 (Q^2), −99 (Q^3), −108 (Q^4) ppm. Porosimetry (nitrogen, 77 K). Specific area: 490 $m^2 \cdot g^{-1}$. Mean pore diameter: 200 Å. SAXS: power law, −3.7; $D_s = 2.3$. $E_{0.6} = 0.20$.

S_6 (THF, HCl). IR (KBr): 946, 1082, 1218, 3510 cm^{-1}. NMR CP-MAS ^{29}Si δ: −91 (Q^2), −100 (Q^3), −109 (Q^4) ppm. Porosimetry (nitrogen, 77 K). Specific area: 460 $m^2 \cdot g^{-1}$. Mean pore diameter: 15 Å. SAXS: power law, −2.5; $D_s = 3.5$(!). $E_{0.6} = 0.22$.

TABLE 7
Yields for the Xerogels ST_{1-6} and $ST'_{3,4}$

Xerogel	Mass of xerogel obtained (g)	Yield (%)
ST_1	1.6	80
ST_2	1.7	85
ST_3	1.7	85
ST'_3	1.7	85
ST_4	1.6	80
ST'_4	1.7	85
ST_5	1.69	84
ST_6	1.7	85

Chemical Treatment

In a typical experiment, the xerogel (1.00 g) was poured into a 50-mL monocol flask, surrounded by a refrigerant. The reagents, solvent (20.0 mL), H_2O (39.0 mL), and an aqueous molar solution of catalyst (0.3 mL, 0.3 mmol) were added. The suspension was heated until methanol reflux for 4 days without stirring. The suspension was then filtered and the residue washed 3 times using 20.0 mL of H_2O, THF, acetone, and diethyl ether and dried for 24 hours under vacuum (2 mmHg) at ambient temperature. For mass and yields see Table 7.

Silica Xerogels Characterization after Chemical Treatment

ST_1 (EtOH, NH_3). IR (KBr): 959, 1082, 1189, 3476 cm^{-1}. NMR CP-MAS ^{29}Si δ: −90 (Q^2), −100 (Q^3), −108 (Q^4) ppm. Porosimetry (nitrogen, 77 K). Specific area: 590 $m^2 \cdot g^{-1}$. Mean pore diameter: 100 Å. SAXS: Porod behavior. $S_p = 650\ m^2 \cdot g^{-1}$. $l_s = 29$. $l_p = 90$. $E_{0.6} = 0.11$.

ST_2 (EtOH, HCl). IR (KBr): 968, 1093, 1218, 3476 cm^{-1}. NMR CP-MAS ^{29}Si δ: −101 (Q^3), −110 (Q^4) ppm. Porosimetry (nitrogen, 77 K). Specific area: 5 $m^2 \cdot g^{-1}$. SAXS: Porod behavior. $S_p = 6\ m^2 \cdot g^{-1}$. $l_s = 3550$. $l_p = 23$. $E_{0.6} = 0.11$.

ST_3 (MeOH, NH_3). IR (KBr): 968, 1098, 1218, 3259, 3466 cm^{-1}. NMR CP-MAS ^{29}Si δ: −91 (Q^2), −100 (Q^3), −109 (Q^4) ppm. Porosimetry (nitrogen, 77 K). Specific area: 300 $m^2 \cdot g^{-1}$. Mean pore diameter: 200 Å. SAXS: Porod behavior. $S_p = 200\ m^2 \cdot g^{-1}$. $l_s = 96$. $l_p = 68$. $E_{0.6} = 0.14$.

ST'_3 (MeOH, NH_3). IR (KBr): 968, 1098, 1186, 3259, 3444 cm^{-1}. NMR CP-MAS ^{29}Si δ: −92 (Q^2), −101 (Q^3), −111 (Q^4) ppm. Porosimetry (nitrogen, 77 K). Specific area:

420 $m^2 \cdot g^{-1}$. Mean pore diameter: 100 Å. SAXS: Porod behavior. $E_{0.6} = 0.11$.

ST_4 (MeOH, HCl). IR (KBr): 971, 1098, 1241, 3475 cm^{-1}. NMR CP-MAS ^{29}Si δ: -90 (Q^2), -100 (Q^3), -110 (Q^4) ppm. Porosimetry (nitrogen, 77 K). Specific area: 5 $m^2 \cdot g^{-1}$. SAXS: Porod behavior. $S_p = 5\ m^2 \cdot g^{-1}$. $l_s = 4087$. $l_p = 22$. $E_{0.6} = 0.13$.

ST_4' (MeOH, HCl). IR (KBr): 955, 1092, 1230, 3486 cm^{-1}. NMR CP-MAS ^{29}Si δ: -92 (Q^2), -101 (Q^3), -110 (Q^4) ppm. Porosimetry (nitrogen, 77 K). Specific area: 1 $m^2 \cdot g^{-1}$. SAXS: power law, -2.7; $D_s = 3.3$ (!). $E_{0.6} = 0.13$.

ST_5 (THF, NH_3): IR (KBr): 954, 1090, 1176, 3340 cm^{-1}. NMR CP-MAS ^{29}Si δ: -92 (Q^2), -101 (Q^3), -109 (Q^4) ppm. Porosimetry (nitrogen, 77 K). Specific area: 360 $m^2 \cdot g^{-1}$. Mean pore diameter: 200 Å. SAXS: power law, -3.6; $D_s = 2.4$. $E_{0.6} = 0.11$.

ST_6 (THF, HCl). IR (KBr): 959, 1093, 1224, 3466 cm^{-1}. NMR CP-MAS ^{29}Si δ: -93 (Q^2), -101 (Q^3), -111 (Q^4) ppm. Porosimetry (nitrogen, 77 K). Specific area: 80 $m^2 \cdot g^{-1}$. Mean pore diameter: 35 Å. SAXS: power law, -3.0; $D_s = 3$. $E_{0.6} = 0.12$.

REFERENCES

1. R. J. P. Corriu, *Angew. Chem., Int. Ed.* **39,** 1376 (2000).
2. R. J. P. Corriu and D. Leclercq, *Angew. Chem., Int. Ed. Engl.* **35,** 4001 (1996).
3. P. Chevalier, R. J. P. Corriu, J. J. E. Moreau, and M. Wong Chi Man, *J. Sol-Gel Sci. Technol.* **8,** 603 (1997).
4. P. Chevalier, R. J. P. Corriu, P. Delord, J. J. E. Moreau, and M. Wong Chi Man, *New J. Chem.* **423** (1998).
5. B. Boury, P. Chevalier, R. J. P. Corriu, P. Delord, J. J. E. Moreau, and M. Wong Chi Man, *Chem. Mater.* **11,** 281 (1999).
6. R. J. P. Corriu, J. J. E. Moreau, P. Thépot, and M. Wong Chi Man, *Chem. Mater.* **4,** 1217 (1992).
7. B. Boury, R. J. P. Corriu, P. Delord, and V. Le Strat, *New J. Chem.* **23,** 531 (1999).
8. A. Bassindale and P. G. Taylor, *in* "The chemistry of organosilicon compounds; part I" (S. Pataï and Z. Rappoport), p 839, Wiley, New York, 1989.
9. C. Chuit, R. J. P. Corriu, C. Reyé, and C. Young, *Chem. Rev.* **93,** 1371 (1993).
10. R. J. P. Corriu, R. Perz, and C. Réye, *Tetrahedron* **39,** 999 (1983).
11. G. Engelhardt and D. Michel, "High-resolution NMR of Silicates and Zeolites." Wiley, Chichester, 1987.
12. H. Marsmann, *in* 17, (P. Dielh, E. Fluck, and R. Kosfeld, Eds), p 65. Springer Verlag, Berlin, 1981.
13. A. Emmerling and J. Fricke, *J. Non-Cryst. Solids* **145,** 113 (1992).
14. R. K. Iler, "The Chemistry of Silica." Wiley, New York, 1979.